Talanta 265 (2023) 124846

Contents lists available at ScienceDirect

Talanta

journal homepage: www.elsevier.com/locate/talanta

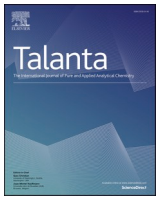

Electrochemical sensing of doxorubicin hydrochloride under sodium alginate antifouling conditions using silver nanoparticles modified glassy carbon electrodes

Elif Lulek [a,1], Jafar Soleymani [b,1], Morteza Molaparast [a], Yavuz Nuri Ertas [a,c,*]

[a] ERNAM – Nanotechnology Research and Application Center, Erciyes University, Kayseri, Turkey
[b] Pharmaceutical Analysis Research Center, Tabriz University of Medical Sciences, Tabriz, Iran
[c] Department of Biomedical Engineering, Erciyes University, Kayseri, Turkey

ARTICLE INFO

Handling Editor: J.-M. Kauffmann

Keywords:
Biomedical analysis
Doxorubicin
Unprocessed plasma
Electrochemical detection
Silver nitrate nanoparticles

ABSTRACT

Doxorubicin (DOX) is a highly effective anticancer drug with a narrow therapeutic window; thus, sensitive and timely detection of DOX is crucial. Using electrodeposition of silver nanoparticles (AgNPs) and electropolymerization alginate (Alg) layers on the surface of a glassy carbon electrode, a novel electrochemical probe was constructed (GCE). The fabricated AgNPs/poly-Alg-modified GCE probe was utilized for the quantification of DOX in unprocessed human plasma samples. For the electrodeposition of AgNPs and electropolymerization of alginate (Alg) layers on the surface of GCE, cyclic voltammetry (CV) was used in the potential ranges of −2.0 to 2.0 V and −0.6 to 0.2 V, respectively. The electrochemical activity of DOX exhibited two oxidation processes at the optimum pH value of 5.5 on the surface of the modified GCE. The DPV spectra of poly(Alg)/AgNPs modified GCE probe toward consecutive concentrations of DOX in plasma samples demonstrated wide dynamic ranges of 15 ng/mL-0.1 μg/mL and 0.1–5.0 μg/mL, with a low limit of quantification (LLOQ) of 15 ng/mL. The validation results indicated that the fabricated electrochemical probe might serve as a highly sensitive and selective assay for the quantification of DOX in patient samples. As an outstanding feature, the developed probe could detect DOX in unprocessed plasma samples and cell lysates without the requirement for pretreatment.

1. Introduction

Doxorubicin (DOX) is a highly effective anticancer medication that has been routinely used for the last three decades. Although DOX has been conclusively shown to be an effective anticancer treatment, it is associated with serious side effects such as cardiac problems, liver damage, and renal toxicity [1,2]. Additionally, DOX's therapeutic use is limited by the accumulation of reactive oxygen species produced by scavenger enzymes, which rapidly contribute to DOX's lethal effect on neoplastic cells. DOX administered intravenously resulted in a lack of customized therapy, inadequate drug transport to the tumor location, and severe patient toxicity. Due to the prevalence of cancer, surveillance and assessment of chemotherapy drugs are essential [3–5].

For DOX detection, several analytical methods are applicable, including liquid chromatography coupled to tandem mass spectrometry, high-performance liquid chromatography, fluorescence probes, electrochemical biosensors, and electrophoresis. Despite the availability of several analytical techniques, electrochemical sensors are favored due to their enhanced analyte detection capabilities, low cost, high stability, and mobility for on-site monitoring [6–8].

Due to the quinone and hydroquinone groups present in DOX, it may be used to assess the electrochemical reduction or oxidation of a medicine. The redox mechanism reduces both the quinone group and the carbonyl side chain, resulting in two sets of reduction waves. This compound might be identified easily using electrochemical methods. In addition to their simplicity, electrochemical techniques possess a high level of selectivity and sensitivity [9,10].

Nanoparticles such as AgNPs have been extensively employed in different disciplines. Advantages include shape diversity, size tunable properties, crystallinity, and ease of synthesis. Diverse shapes of Ag

* Corresponding author. ERNAM—Nanotechnology Research and Application Center, Erciyes University, Kayseri, 38039, Turkey.
E-mail address: yavuzertas@erciyes.edu.tr (Y.N. Ertas).
URL: http://www.ertaslab.com (Y.N. Ertas).
[1] equal contribution.

https://doi.org/10.1016/j.talanta.2023.124846
Received 23 February 2023; Received in revised form 24 May 2023; Accepted 19 June 2023
Available online 24 June 2023

nanomaterials were applied to develop various sensing platforms [11–13].

Electrochemical polymerization, also known as electropolymerization, is a technique for modifying the surface of an electrode in which a thin layer of polymer films is produced under an electrochemical condition using predominantly potentiostatic (constant potential) or potentiodynamic (linearly scanned potential) techniques [14]. During the electropolymerization of alginate (Alg), a thin layer of polyalginate is produced, which provides a secondary surface for the functional groups of analytes to interact [15,16].

Electrodeposition of Alg and AgNPs on the surface of GCE was used to construct a novel electrochemical probe. AgNPs and Alg enhance the interaction between electrode and analyte, respectively, by increasing the geometrical surface of the GCE and the interaction between electrode and analyte. In addition, Alg molecules serve as an antifouling agent by filtering the interfering chemicals that might reach the modified electrode's surface and deactivate or impair its electroanalytical characteristics. The constructed AgNPs/Alg-based sensor exhibited considerable DOX oxidation electrochemical activity. The antifouling activity of the Alg can definitely boost the sensitivity of the constructed platform.

2. Experimental

2.1. Chemicals and reagents

DOX, silver nitrate ($AgNO_3$), sodium dihydrogen phosphate, disodium hydrogen phosphate, Alg, hydrochloric acid, sodium hydroxide, and sulfuric acid were purchased from Sigma Aldrich (Germany) 50mM of phosphate buffer was prepared by using NaH_2PO_4 and Na_2HPO_4 salts. Also, a stock solution of DOX with a concentration of 250 μg/mL was prepared by dissolving an appropriate mass of DOX in PBS solution (0.1 M, pH = 5.5). Also, $AgNO_3$ and Alg solutions were prepared with concentration of 0.01 and 1 M, respectively. All substances were prepared in deionized water and then stored in a refrigerator and dark place. Frozen blank plasma samples were obtained from Erciyes University Medical Hospital.

2.2. Apparatus and measurements

This study was conducted using the AUTOLAB electrochemical system, where the system was connected to an electrochemical cell and a laptop running the Nova 2.1 software. As reference electrodes, an Ag/AgCl electrode and a platinum electrode were used. As the working electrode, a GCE electrode (d = 2 mm) manufactured by Azar Electrode Company (Urmia, Iran) was utilized. The spectrum was recorded using differential pulse voltammetry (DPV), with a potential range of −0.6 to 0.2 V, a modulation amplitude of 0.025 V, a modulation period of 0.05 s, a time interval of 0.5 s, and a scan rate of 0.01 V/s. The surface morphology of the GCE electrode was examined using a high-resolution field emission scanning electron microscope to identify silver nanoparticles and polymerization (Field emission scanning electron microscopy (FE-SEM; ZEISS, GEMINI 500). Coated elements on the electrode were observed by energy dispersive spectroscopy (EDS). Finally, microscopic fluorescent tests were observed under a microscope.

2.3. Sensor design

2.3.1. Electrode pretreatment and cleaning

At the first step, bare electrodes were cleaned as follows: Firstly, the GCE electrode was physically cleaned by polishing on a pad, followed by inserting it into the acetone and water/acetone mixtures, and finally washing with pure water. To continue the cleaning process, the electrode was inserted in an acidic solution containing H_2SO_4 (50 mM)/HNO_3 (50 mM) for at least 10 min and finally washed with pure water and dried at room temperature. To further clean these electrodes, they were immersed in H_2SO_4 (100 mM), and the CV technique was employed for 20 cycles in the potential range between −1.0 and 1.0 V to observe repetitive CVs.

2.3.2. Synthesis of AgNPs on the surface of GCE by electrodeposition technique

As prepared bare electrode surface was modified by AgNPs. Firstly, $AgNO_3$ (0.05 mM) was added to the electrochemical cell, and CV technique was used to electrochemically synthesize and deposit AgNPs on the GCE surface at −0.8 to 0.5 V potential range with total cycles of 30 and a scan rate of 100 mV/s against the Ag/AgCl reference electrode. Fig. 1a demonstrates the CVs of the electro-synthesis of AgNPs on a typical GCE.

2.3.3. Electrodeposition of Alg on the surface of AgNPs modified GCE

In a cell containing Alg at a concentration of approximately 5 mM (pH = 5.5), AgNPs-modified GCE was introduced. The electropolymerization of Alg on the surface of AgNPs/GCE was afterwards accomplished using CV technique. CV was executed at a possible range of −2.0 to 2.0 V and 20 cycles. Fig. 1b represents the electrodeposition of Alg on the AgNPs/GCE.

2.4. Cell culture and biological tests

2.4.1. General cell culture procedure

MDA-MB-231 (human breast cancer cells) were seeded into T-75 mL cell culture flasks that had previously been filled with RPMI media supplemented with 10% FBS and 1% penicillin/streptomycin and incubated at 37 °C (5% CO_2 atmosphere). The cells were isolated after the majority of the bottom of the flask was filled with trypsin 1X. After rinsing the flask with PBS and inactivating it with 3 mL of trypsin culture medium, 1 mL of trypsin was applied to the flask, and the separated cells were put into 15 mL of Falcon and centrifuged. The appropriate amount of cells was then added to the flask, and 14 mL of complete culture medium was added and kept in the incubator for further testing.

2.4.2. Fluorescence imaging of the cell uptake of DOX

A total of 500,000 cells were seeded into each well of the six-well plate for fluorescence imaging purposes. After overnight incubation, the cells were treated with several concentrations of dox (1 ppm, 5 ppm, 10 ppm, 15 ppm, and 20 ppm), and the supernatant was removed after 2 h to determine the quantity of dox left in the medium and analyzed using a newly constructed biosensor. Finally, fluorescence microscopy was used to analyze cancer cells.

2.4.3. Determination of DOX in cell lysates

In the preceding phase, DOX-containing media were extracted from cancer cells and prepared for analysis using the newly developed electrochemical approach. Then, 1 mL of the medium was transferred into the working cell of the electrochemical device and determined using the DPV method, and the unreacted DOX concentrations were calculated using the collected data.

3. Results and discussions

3.1. Electrode modification and characterization of AgNPs and Alg modified GCE

The CV technique was utilized for the surface improvement of the GCE surface. AgNPs were electrodeposited on the surface of GCE by *in situ* reduction of Ag (I) ions. *In situ* synthesis generates a reproducible monolayer of AgNPs on the GCE surface. In addition, CV-based electrodeposition of AgNPs enables the control of particle sizes and prevents the aggregation of the nanoparticles, providing constant electrodeposition of AgNPs. As seen in Fig. 1a, peak currents of CVs have increasing (in oxidation) and decreasing (in reduction) trends with increasing CV

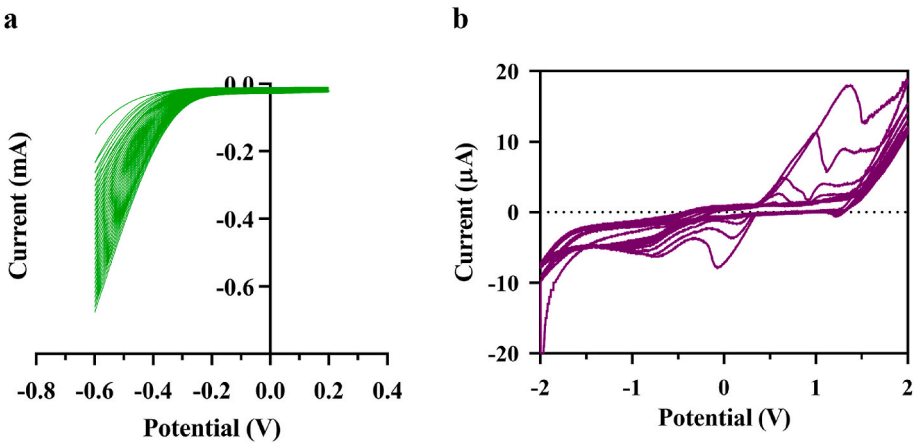

Fig. 1. (a) CVs for AgNPs electrodeposition on the GCE surface at − 0.8 to 0.5 V (N = 30 cycles, Scan rate = 50 mV/s), (b) CVs of electropolymerization of Alg on the surface AgNPs modified GCE (N = 20 cycles, Scan rate = 100 mV/s).

scans, forming an electroconductive nanolayer of AgNPs on the GCE surface.

As the second step, Alg molecules were polymerized on the AgNPs layer. Electropolymerization of Alg through the CV technique provides the possibility to regulate the physicochemical properties of the electrode surface by tuning scanning factors such as cycle number, potential scan rate, and potential amount. From Fig. 1b, it is obvious that both cathodic and anodic currents are enhanced with increasing cycle numbers, confirming the increased surface conductivity of the modified electrode. However, conductivity and current are achieved at a specific scan rate, which we propose as the optimum scan rate for algae electrodeposition. Furthermore, upon the growth of the Alg biopolymer layers, more prolonged 3D networks of delocalized electrons are produced on the surface of GCE, which can result in a decrease in oxidation potential.

Typically, polysaccharide electrodeposition mechanisms use elec-

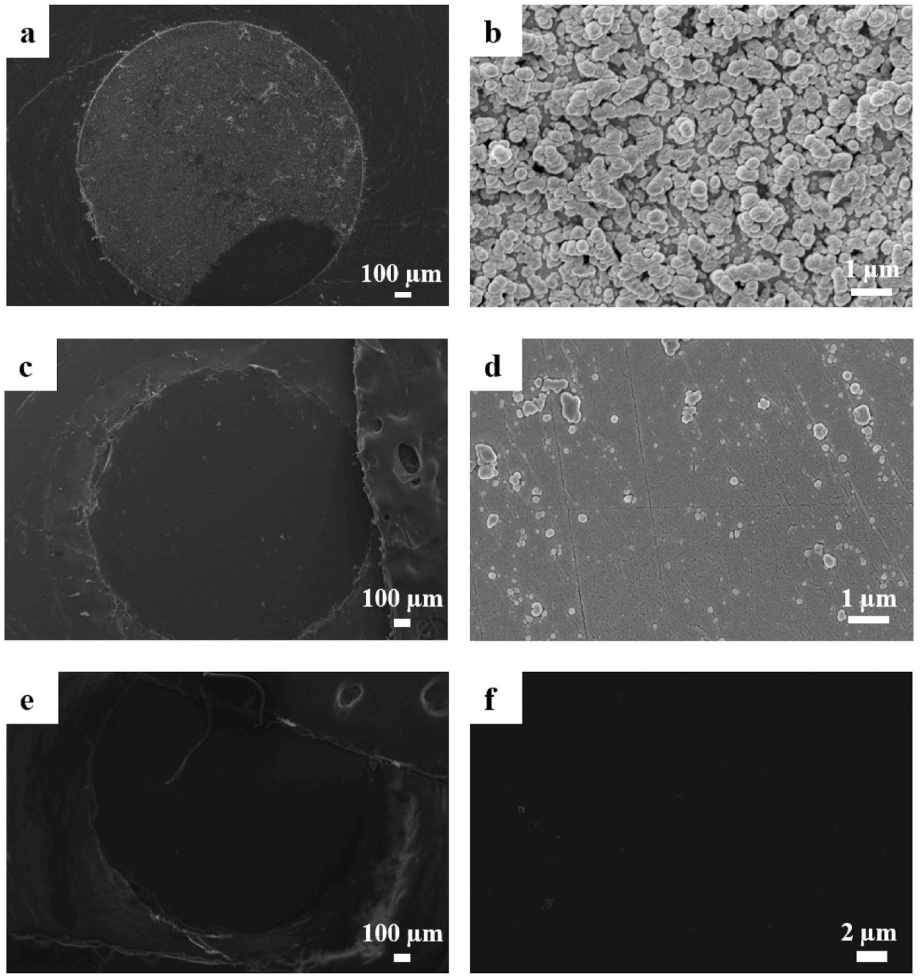

Fig. 2. SEM images at different magnifications. (a, b) AgNPs/GCE surfaces, (c, d) poly-HAlg/AgNPs/GCE, and (e, f) bare GCE in altered scales.

trochemical reactions to generate pH gradients that cause polysaccharide to locally neutralize and produce a polysaccharide hydrogel film on the electrode surface via a reversible sol-gel transition [15]. Alg electropolymerization mechanism could be explored in several consecutive steps. At the first step, water molecules are electrolyzed to locally produce hydronium ions, and then they are reacted Alg, and (iii) at the low pH region, a layer of alginic acid (HAlg) gel is produced around the electrode [17].

$$H_2O \rightarrow O_2 + 2H^+ + 2e^- \quad (1)$$

$$Na \cdot Alg \rightarrow Na^+ + Alg^- \quad (2)$$

$$Alg^- + H^+ \rightarrow HAlg \quad (3)$$

It is noteworthy that electrophoretic motion of ionic particles results in the increasing of the number of particles close to the electrode surface; this does not mean that a film is produced on the electrode surface. To confirm the formation of a HAlg layer on the surface of AgNPs/GCE, SEM images are needed. Fig. 2 demonstrates SEM images of the bare GCE, GCE/AgNPs, and GCE/AgNPs/Alg. As seen, the bare GCE surface morphology is plain while GCE/AgNPs produce AgNPs with varied shapes on the electrode, representing effective electrodeposition of AgNPs. After electropolymerization of Alg macromolecules on the GCE/AgNPs, a 3D compact layer is produced that contains various cavities to act as a sieve to filter fouling agents and allow DOX molecules to cross and reach the electrode surface and electrochemically react.

3.2. Electrochemical behavior of poly-HAlg/AgNPs/GCE platform towards DOX

Electrochemical behavior of the poly-HAlg/AgNPs/GCE platform towards DOX was explored using the CV technique, which provides valuable information about the developed electrode function in the presence and absence of DOX. Fig. 4a represents CV voltammograms of poly-HAlg/AgNPs/GCE and bare GCE in the presence and absence of DOX (2.5 mg/L) in the supporting phosphate buffer solution (pH = 5.5) at a −1.0 to +1.0 V potential range and scan rate of 100 mV/s. As can be seen, bare GCE exhibit no significant electrochemical activity. While upon modification with AgNPs, the conductivity of the electrode surface is increased, and two peaks are obtained at 0.45 V and 0.11 V, as anodic and cathodic peaks, respectively. AgNPs promote the effective surface area for the next electropolymerization of Alg on the electrode surface. After electropolymerization of Alg on the surface of AgNPs/GCE, two peaks are observed at +0.37 and + 0.5 V as anodic peaks.

The comparison of CVs of AgNPs/GCE and poly-HAlg/AgNPs/GCE indicates that the peak current of poly-HAlg/AgNPs/GCE is logically decreased as a result of the attachment of an organic layer, i.e., Alg (as a macromolecule with low electron conductivity). However, in the presence of DOX, a new anodic peak at −0.55 V and two cathodic peaks around 0.39 V and −0.59 V are observed, which are attributed to the oxidation and reduction of DOX, respectively. It is noteworthy that another anodic peak is expected to be observed around 0.45 V; however, this peak is already overlapped with the oxidation peak of HAlg. AgNPs exhibit an anodic peak at a potential of around 0.2 V as an oxidation peak, which relates to the electrochemical oxidation of the Ag° to Ag^+ [18].

Regarding the obtained results, a potential of around −0.5 V was selected as the analytical peak of DOX for the next optimization and validation steps. Generally, negative potentials are advantageous because of the low interference of biological media in that potential range. A literature review showed that DOX has two main reversible oxidation peaks at around −0.5 and + 0.5 V, relating to the two hydroxyl groups of the hydroquinone structure of DOX (Fig. 3).

3.3. Effect of pH

The electrochemical behavior of DOX is strongly affected by the pH of the medium, which is mainly caused by the hydroquinone structure of DOX. The influence of the pH on the peak current and potential was investigated using CV and DPV techniques. Fig. 4b and c shows the CVs and DPVs in the pH range of 2.5–10.5. It was found that with increasing pH, the oxidation peak potential of DOX shifts to more negative potentials. The Epa vs. pH relationship can be demonstrated by the following equation (Fig. 4d).

$$E_{pa}(V) = -0.05566\ pH - 0.2120, R^2 = 0.9744 \quad (4)$$

The slope E_{pa} *vs.* pH of 0.05566 V/pH is so close to the theoretical value of 0.0592 V/pH, proposing that equal numbers of protons and electrons are applied in the electro-oxidation of DOX with a reversible transfer. It was also found that the anodic peak current (Ipa) of poly (Alg)/AgNPs/GCE towards DOX oxidation was greatest at pH = 5.5. As a result, pH = 5.5 was chosen as the optimum pH for the next steps.

3.4. Kinetic study of the oxidation of DOX

The CV technique is used to investigate the mechanism of oxidation/reduction of any analyte on the electrode surface. An increasing trend is observed during enhancement of the scan rate, where faster scan rates decrease the diffusion layer size and, as a result, higher peak currents are obtained [19]. At various scan rates, the electrochemical CVs of the poly (Alg)/AgNPs/GCE electrode were recorded in the presence of DOX (2.5 mg/mL). Fig. 5a shows typical CVs of poly(Alg)/AgNPs/GCE in the presence of DOX at various scan rates.

The oxidation peak of DOX is observed around −0.5 V at diverse scan rates from 20 mV/s to 1000 mV/s, and the intensity of the oxidation peak is enhanced with increasing scan rates (Fig. 5a). A linear relationship is constructed between peak current and scan rates (Fig. 5b), confirming a surface-determined progression of electron transfer between the poly(Alg)/AgNPs/GCE electrode and electrolyte. The I_{pa} *vs.* ν for DOX oxidation could be presented as I_{pa} (μA) = 8.800ν - 0.4642 with R-square of 0.9965.

To determine whether the DOX electrochemical reaction was reversible or irreversible, Epa vs. ln was plotted from 550 to 950 mV/s in 50 mM of PBS (pH = 5.5). If potential of peak is meaningfully dependent on sweep rate, it means that the electrochemical reaction has an irreversible process. In the poly(Alg)/AgNPs/GCE electrode, the E_{pa} was

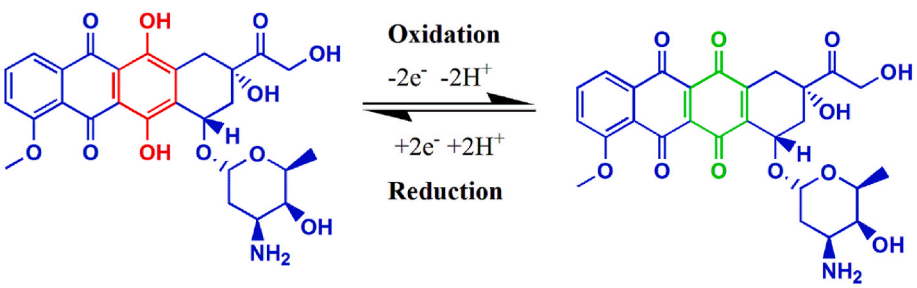

Fig. 3. Oxidation mechanism of DOX on poly(Alg)/AgNPs/GCE.

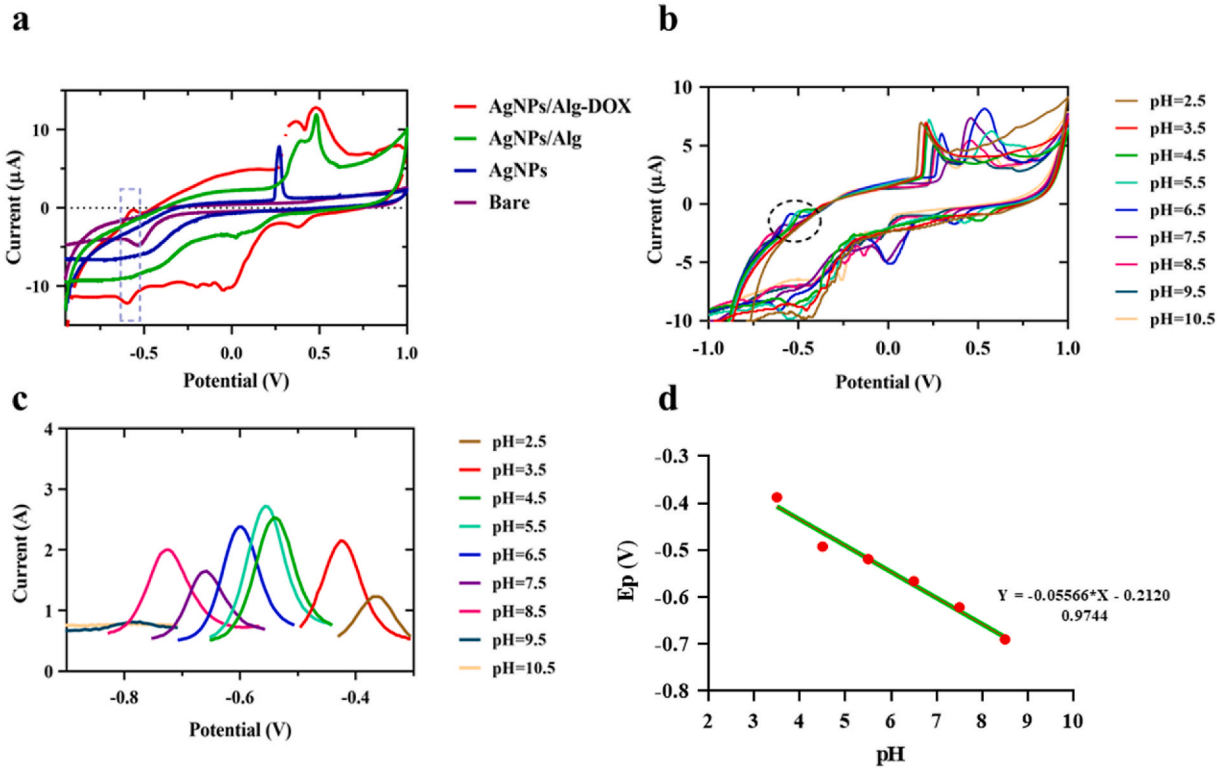

Fig. 4. (a) CVs of absence and presence of DOX (2.5 mg/L). (PBS buffer: 50 mM M, pH = 6.5, scan rate 100 mV/s), (b) CVs, (c) DPVs of poly(Alg)/AgNPs/GCE at various pHs from 2.5 to 10.5, and (d) Epa vs. pH curve for the oxidation of DOX. (PBS, 50 mM, potential range – 1.0 to 1.0 V, scan rate 50.

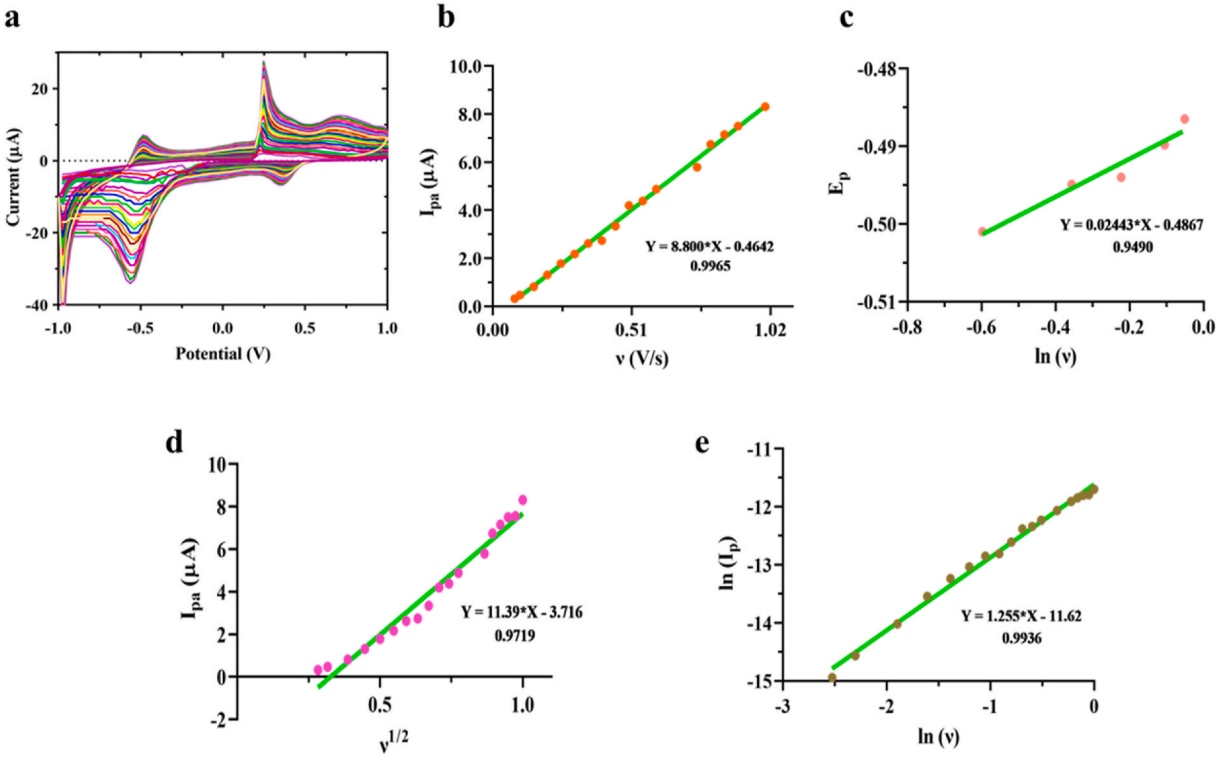

Fig. 5. (a) Scan rate spectra, (b) Ipa vis. ν, (c) Ep vis. ln (ν), (d) Ipa vis. ν0.5, and (e) ln(Ipa) vis. ln (ν) of poly(Alg)/AgNPs/GCE (PBS, 50 mM, potential range – 1.0 to 1.0 V, DOX, 2.5 mg/L). mV/s, DOX, 2.5 mg/L).

proportionally changed with increasing ln ν. As shown in Fig. 5c, there is a proportional relationship between E_{pa} and ln ν. By increasing the scan rate, the oxidation peak potential of DOX is moved to more positive peak potentials. E_{pa} *vs.* ln ν equation could be presented as: $E_{pa}(V) = 0.02443$ ln ν (Vs^{-1}) – 0.4867 with $R^2 = 0.95$. According to Laviron's theory, the relationship between E_{pa} and scan rate could be expressed by the

following equation:

$$E_{Pa} = E_0 + \frac{RT}{\alpha nF} ln\left(\frac{RTk^{\circ}}{\alpha nF}\right) + \frac{RT}{\alpha nF} lnv \quad (5)$$

here, T, n, R, and F are temperature (K), the number of electron transfers, gas constant (R = 8.314 J mol^{-1} K^{-1}), and Faraday constant (F = 96,493C mol^{-1}), respectively. Also, α, k°, and E_0 denote the electron transfer coefficient, standard rate constant of the reaction, and formal potential, respectively. Regarding Eq. 2, the αn can be simply estimated by the E_{pa} *vs.* ln *ν* slope. αn_a was calculated to be 1.05. Thus, the number transferred electrons was calculated as 2.10 for DOX. It is noteworthy that E_{pa} is dependent on scan rate in the irreversible electrochemical reactions; therefore, it can be concluded that the DOX oxidation reaction is an irreversible electrochemical reaction.

To check the mechanism of oxidation of DOX on the poly(Alg)/AgNPs/GCE, I_{pa} *vs.* *ν* and I_{pa} *vs.* $\nu^{0.5}$ were plotted (Fig. 5b and d). Results revealed that both of the plots are linear in the investigated scan rate range. However, in I_{pa} *vs.* $\nu^{0.5}$ plot, the intercept is near to zero, proposing adsorption-controlled oxidation of DOX on the poly(Alg)/AgNPs/GCE. This finding was further supported by the ln(I_{pa}) *vs.* ln(*ν*) equation, i.e., ln(I_{pa}) = 1.255 ln *ν*-11.2 with R^2 of 0.9936 (Fig. 5e). It is noteworthy that the slope of by ln(I_{pa}) *vs.* ln(*ν*) is close to 1.0 in the adsorption-controlled oxidation mechanisms.

The surface coverage of DOX (Γ* as mol cm^{-2}) was also calculated using Faraday's law and plotting I_{pa} *vs.* *ν* [20].

$$l_p = \frac{nFQv}{4RT} = \frac{n^2F^2A\Gamma^{*}\nu}{4RT} \quad (6)$$

in this equation, n, *ν*, A, and Γ* represent the number of electrons, scan rate, electrode surface area, and DOX surface concentration, respectively. In this work, the amounts of n and A are equal to 2, 3.14 × 10^{-2} cm^2, respectively. Γ* is calculated as 7.45 × 10^{-5} mol cm^{-2} for poly (Alg)/AgNPs modified GCE electrode, indicating efficient adsorption of DOX on the surface of the modified electrode.

3.5. Analytical performance

3.5.1. Calibration curve

AgNPs were utilized in this study as a promising electrochemical sensor for detecting doxorubicin levels in patient plasma. The current study fabricates a unique electrochemical sensor utilizing AgNPs electropolymerized on the surface of GCE. The surface of GCE was altered by the addition of AgNPs since any increase in the geometrical surface area has the potential to result in increased sensitivity. The surface of GCE was altered by the addition of AgNPs since any increase in the geometrical surface area has the potential to result in increased sensitivity. The detection parameters of the poly(Alg)/AgNPs modified GCE electrode platform were calculated using the DPV technique by plotting a calibration curve. Upon an increase in the DOX concentration, the probe current is increased linearly. The DPV spectra of the poly(Alg)/AgNPs modified GCE probe toward successive concentrations of DOX in plasma samples are shown in Fig. 6a. The developed probe exhibited wide dynamic linearity at two ranges of 15 ng/mL–0.1 μg/mL and 0.1–5.0 μg/mL. The low limit of quantification (LLOQ) was reported as 15 ng/mL (Fig.6b). The developed sensor demonstrated a broad linear response and a low detection limit to determine DOX in human blood samples.

Table 1 lists the analytical performances, materials, and applied techniques of the reported electrochemical methods for the quantification of DOX in biological fluids. This probe can detect DOX concentrations as low as the reported method, and it can also detect DOX in unprocessed plasma samples. Generally, methods with minimal

Table 1
Analytical figures-of-merit of the reported electrochemical methods for the detection of DOX in human samples.

Electrode	Technique	Dynamic range	LOD/ LLOQ	Media	Ref.
TiO_2/nafion composite	CV	5–2000 nM	1 nM	Plasma	[23]
GQD	DPV	0.018–3.60 μM	0.016 μM	Plasma	[24]
Poly-L-lysine/ MWNTs	SWV	0.0025–0.25 μM	1.0 nM	Whole Blood	[25]
MWCNTs	SWV	0.04–90 μM	0.0094 μM	Serum urine	[26]
$CoFe_2O_4$/ MNPs	DPV	0.05–1150 nM	10 pM	Serum urine	[27]
MWCNTs/Pt	CV	0.05–4.0 μM	0.002 μg/mL	Plasma	[28]
PS/Fe_3O_4-GO-SO_3H	DPV	0.043–3.5 μM 0.026–3.5 μM 0.86–13.0 μM	0.0049 μM 0.0043 μM 0.014 μM	Plasma Urine CF	[29]
PARG	DPV	0.069–1.08	LLOQ: 0.069 nM	Whole Plasma	[29]
PTB	DPV	340–8.6	LLOQ: 0.34 nM	Whole Plasma	[30]
Poly(Alg)/ AgNPs	DPV	15 ng/mL – 0.1 μg/mL and 0.1–5.0 μg/mL	LLOQ: 15 ng/ mL	Plasma	This work

SWV; square-wave voltammetry, DPV; differential-pulse voltammetry, GQDs; graphene quantum dots, MWNTs; multi-walled carbon nanotube, GO; graphene oxide, MNPs; magnetic nanoparticles, PS; polystyrene, PTB; polytoluidine blue, PARG; poly arginine.

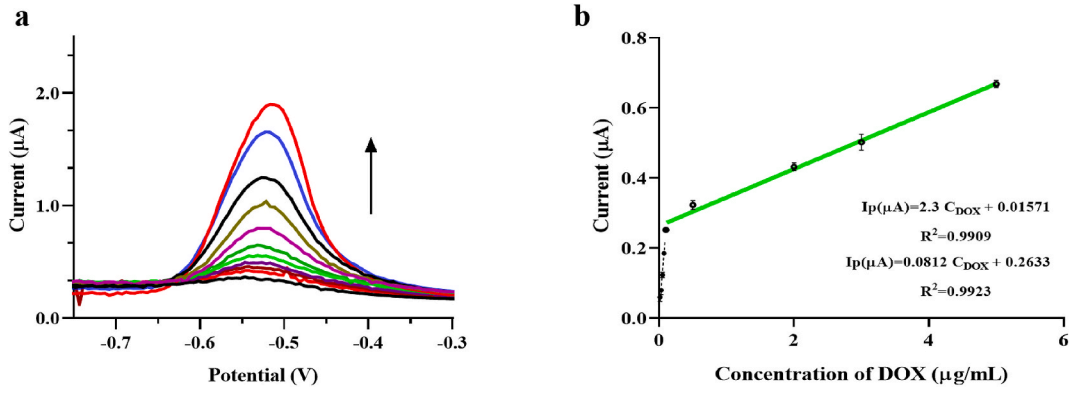

Fig. 6. (a) DPVs of poly(Alg)/AgNPs modified GCE, and (b) calibration curve of different concentrations of DOX in unprocessed plasma media (PBS, 50 mM, pH = 6.5).

pretreatment steps are welcomed in clinics due to their cheapness, fast analysis time, and user-friendly procedure [20–22].

3.6. Method validation

3.6.1. Accuracy, inter-day and intra-day repeatability

The precision of the developed approaches is usually expressed by their intra- and inter-day repeatabilities. Two levels of DOX concentrations from the calibration range were selected to evaluate the intra-day and inter-day precisions. Table 2 collects the obtained inter-day and intra-day repeatability results. Also, the accuracy of the developed method was determined in plasma media. The obtained data points revealed the acceptable precision and accuracy of the method. The repeatability data points, which is expressed in relative standard deviation (RSD%), varied between 1.3 and −15.6%, and the accuracy percentages are expressed in relative error (RE%) and were +5.3 to −4.5% with recoveries from 95.5% to 105.3%. The outcomes proposed that this method is able to analyze DOX in plasma samples with reliable results.

3.6.2. Specific manner of the developed method toward DOX detection

The specificity of the modified electrode over the available possible interfering agents was also investigated. For this purpose, some biomolecules (L-cystein, arginine, tyrosine) and ions (sodium, potassium, chloride, calcium, etc.) were regarded as the electrochemical signal-interfering substances. The signal of the probe was checked in the presence and absence of the substances. The findings revealed that this probe shows acceptable performance toward the detection of DOX, which is mainly caused by the exceptional peak potential and the application of antifouling Alg macromolecules for the fabrication of the probe (Fig. 7).

3.7. Applications of the AgNPs/p-Alg modified GCE probe

3.7.1. Detection of DOX in cell lysates samples

The use of the AgNPs/p-Alg modified GCE probe was investigated in cell lysates at various times of incubation and concentrations. Fig. 8a and b shows the obtained results. Upon increasing the concentration of the DOX, the signal of the probe is enhanced, and as the time of incubation progresses, the electrochemical signal is diminished. These findings are clearly supported by fluorescence microscopic images shown in Fig. 8c and d.

3.7.2. Detection of DOX in real plasma samples

The developed probe was also utilized to detect DOX in patients' plasma samples. No further steps were taken to determine DOX in plasma samples. Firstly, plasma samples were centrifuged, and then about 0.5 mL of plasma and 4.5 mL of buffer solution were added to the reaction cell. DPV measurement was applied to the quantitative determination of DOX in plasma real-time samples. From the obtained results (Table 3), it is obvious that the developed probe can easily detect DOX in the complicated plasma samples with high accuracy.

4. Conclusion

In this work, an innovative electrochemical sensor based on AgNPs deposited on the surface of GCE was developed for the detection of DOX as a chemotherapy drug. This modified electrode is simple and inexpensive to prepare. In addition, this electrode was used for electrochemical measurements of DOX, and it was found that the suggested method had a number of benefits, including rapid electron transfer processes and high stability. The proposed sensor showed excellent selectivity, repeatability, and reproducibility, as well as a low limit of detection and a wide linear range, for the determination of DOX in a real sample. More importantly, this sensor was used for the direct detection of DOX in real samples without the need for extraction or pretreatment. This sensor has promising applications for the determination of trace amounts of DOX in unprocessed human samples and cell lysate in the absence of sophisticated pretreatments and interference from common species seen in real samples. The electrochemical electrode has overall demonstrated the detection of DOX in actual blood samples, and this, together with the advantages outlined above, makes its clinical use highly attractive. In addition, for therapeutic applications, the capacity to detect very low, minimal doses in patients receiving DOX will allow patients to be placed on a regular chemotherapy cycle, therefore boosting the treatment's efficacy and ensuring that patients receive just the essential doses. Consequently, drug-induced damage to patients will be minimized, resulting in highly beneficial therapeutic outcomes.

Table 2
Accuracy, interday- and intraday precision of the developed electrochemical method for the detection DOX in plasma samples.

Nominal concentration (g/mL)	Intraday precision (RSD%)	Interday precision (RSD%)	Interday accuracy (RE %)	Recovery (%)
0.1	1.3	+12.0	+5.3	105.3
2.0	11.9	−15.6	−4.5	95.5

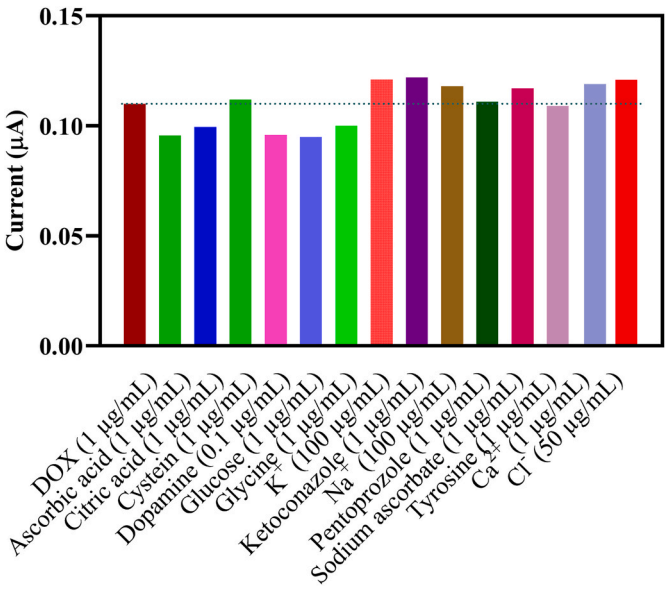

Fig. 7. The effect of several common interfering agents on the detection of DOX in plasma samples.

Author contribution

Elif Lulek: Data curation, Formal analysis, Visualization. Jafar Soleymani: Conceptualization, Formal analysis, Writing – original draft. Morteza Molaparast: Data curation. Yavuz Nuri Ertas: Conceptualization, Formal analysis, Visualization, Supervision, Resources, Writing – original draft, Writing- Reviewing and Editing, Funding acquisition.

Ethical considerations

This study was approved by the Ethics Committee of the Erciyes University (# 96681246), and the study participants signed an informed consent.

Declaration of competing interest

The authors declare the following financial interests/personal relationships which may be considered as potential competing interests: Yavuz Nuri Ertas reports financial support was provided by Erciyes

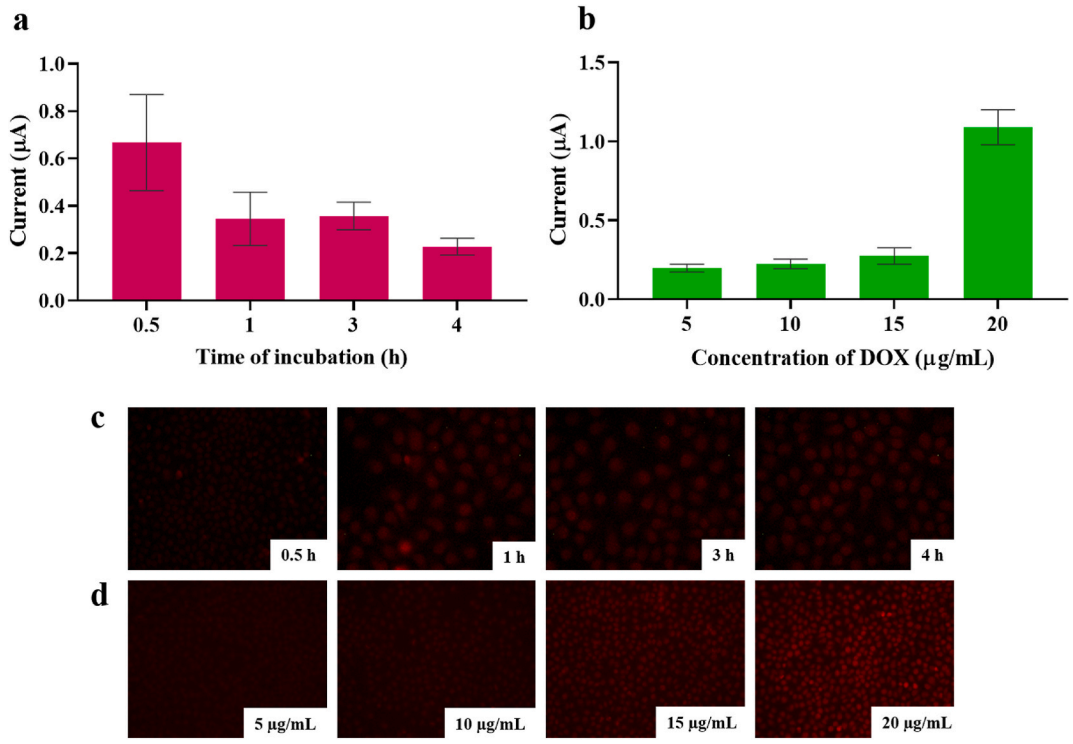

Fig. 8. (a) Incubation of the MCF 7 cell with DOX at various times, (b) various concentrations, (c) fluorescence microscopy images at various incubation times, and (d) concentrations.

Table 3
Determination of DOX in patient samples after 2 h of intake.

Sample No.	Sexuality	Age (year)	Prescribed dose (mg)	Detected concentration (mg/L)
1	Male	66	82	0.023
2	Female	72	91	0.046

University.

Data availability

Data will be made available on request.

Acknowledgments

This work was supported by the Research Fund of the Erciyes University (Project Number FBG-2021-11326).

References

[1] J.A. Sparano, U. Malik, L. Rajdev, C. Sarta, U. Hopkins, A.C. Wolff, Phase I trial of pegylated liposomal doxorubicin and docetaxel in advanced breast cancer, J. Clin. Oncol. 19 (2001) 3117–3125, https://doi.org/10.1200/JCO.2001.19.12.3117.

[2] M. Hashemi, F. Ghadyani, S. Hasani, Y. Olyaee, B. Raei, M. Khodadadi, M. F. Ziyarani, F.A. Basti, A. Tavakolpournegari, A. Matinahmadi, S. Salimimoghadam, A.R. Aref, A. Taheriazam, M. Entezari, Y.N. Ertas, Nanoliposomes for doxorubicin delivery: reversing drug resistance, stimuli-responsive carriers and clinical translation, J. Drug Deliv. Sci. Technol. 80 (2023), 104112, https://doi.org/10.1016/j.jddst.2022.104112.

[3] M. Ashrafizadeh, A. Zarrabi, H. Karimi-Maleh, A. Taheriazam, S. Mirzaei, M. Hashemi, K. Hushmandi, P. Makvandi, E. Nazarzadeh Zare, E. Sharifi, A. Goel, L. Wang, J. Ren, Y. Nuri Ertas, A.P. Kumar, Y. Wang, N. Rabiee, G. Sethi, Z. Ma, Nano)platforms in bladder cancer therapy: challenges and opportunities, Bioeng Transl Med 8 (2023), https://doi.org/10.1002/btm2.10353.

[4] N. Jan, A. Madni, S. Khan, H. Shah, F. Akram, A. Khan, D. Ertas, M.F. Bostanudin, C.H. Contag, N. Ashammakhi, Y.N. Ertas, Biomimetic cell membrane-coated poly (lactic-co-glycolic acid) nanoparticles for biomedical applications, Bioeng Transl Med (2022), https://doi.org/10.1002/btm2.10441.

[5] H.S. Yoo, T.G. Park, Folate-receptor-targeted delivery of doxorubicin nano-aggregates stabilized by doxorubicin–PEG–folate conjugate, J. Contr. Release 100 (2004) 247–256, https://doi.org/10.1016/j.jconrel.2004.08.017.

[6] M. Hasanzadeh, M. Feyziazar, E. Solhi, A. Mokhtarzadeh, J. Soleymani, N. Shadjou, A. Jouyban, S. Mahboob, Ultrasensitive immunoassay of breast cancer type 1 susceptibility protein (BRCA1) using poly (dopamine-beta cyclodextrine-Cetyl trimethylammonium bromide) doped with silver nanoparticles: a new platform in early stage diagnosis of breast cancer and effici, Microchem. J. 145 (2019) 778–783, https://doi.org/10.1016/j.microc.2018.11.029.

[7] Y. Zare, J. Soleymani, M. Rahimi, Y. Nuri Ertas, S. Jafarzadeh, Trends in advanced materials for the fabrication of insulin electrochemical immunosensors, Chem. Pap. 76 (2022), https://doi.org/10.1007/s11696-022-02416-5.

[8] M. Abbasi, M. Ezazi, A. Jouyban, E. Lulek, K. Asadpour-Zeynali, Y.N. Ertas, J. Houshyar, A. Mokhtarzadeh, J. Soleymani, An ultrasensitive and preprocessing-free electrochemical platform for the detection of doxorubicin based on tryptophan/polyethylene glycol-cobalt ferrite nanoparticles modified electrodes, Microchem. J. 183 (2022), https://doi.org/10.1016/j.microc.2022.108055.

[9] B. Khalilzadeh, N. Shadjou, G.S. Kanberoglu, H. Afsharan, M. de la Guardia, H. N. Charoudeh, A. Ostadrahimi, M.-R. Rashidi, Advances in nanomaterial based optical biosensing and bioimaging of apoptosis via caspase-3 activity: a review, Microchim. Acta 185 (2018), https://doi.org/10.1007/s00604-018-2980-6.

[10] M. Hasanzadeh, B. Khalilzadeh, N. Shadjou, G. Karim-Nezhad, L. Saghatforoush, I. Kazeman, M.H. Abnosi, A new kinetic-mechanistic approach to elucidate formaldehyde electrooxidation on copper electrode, Electroanalysis 22 (2010) 168–176, https://doi.org/10.1002/elan.200900294.

[11] J. Zheng, J. Bai, Q. Zhou, J. Li, Y. Li, DNA-templated in situ growth of AgNPs on SWNTs : a new approach for highly sensitive SERS assay of microRNA, Chem. Commun. 51 (2015) 6552–6555, https://doi.org/10.1039/C5CC01003A.

[12] M. Farrokhnia, S. Karimi, S. Askarian, Strong hydrogen bonding of gallic acid during synthesis of an efficient AgNPs colorimetric sensor for melamine detection via dis-synthesis strategy, ACS Sustain. Chem. Eng. 7 (2019) 6672–6684, https://doi.org/10.1021/ACSSUSCHEMENG.8B05785/SUPPL_FILE/SC8B05785_SI_001.PDF.

[13] A. Saenchoopa, W. Boonta, C. Talodthaisong, O. Srichaiyapol, R. Patramanon, S. Kulchat, Colorimetric detection of Hg(II) by γ-aminobutyric acid-silver nanoparticles in water and the assessment of antibacterial activities, Spectrochim. Acta Mol. Biomol. Spectrosc. 251 (2021), 119433, https://doi.org/10.1016/J.SAA.2021.119433.

[14] J. Soleymani, M. Hasanzadeh, M. Eskandani, M. Khoubnasabjafari, N. Shadjou, A. Jouyban, Electrochemical sensing of doxorubicin in unprocessed whole blood, cell lysate, and human plasma samples using thin film of poly-arginine modified glassy carbon electrode, Mater. Sci. Eng. C 77 (2017) 790–802, https://doi.org/10.1016/j.msec.2017.03.257.

[15] Y. Cheng, X. Luo, J. Betz, G.F. Payne, W.E. Bentley, G.W. Rubloff, Mechanism of anodic electrodeposition of calcium alginate, Soft Matter 7 (2011) 5677–5684, https://doi.org/10.1039/c1sm05210a.

[16] P. Vanessa, D. Da, M. Sola-penna, M. Farina, L. Rodrigues, A. Yoshihaki, M. H. Rocha-leão, Biointerfaces Microcapsules of alginate/chitosan containing magnetic nanoparticles for controlled release of insulin, Colloids Surf. B Biointerfaces 81 (2010) 206–211, https://doi.org/10.1016/j.colsurfb.2010.07.008.

[17] M. Cheong, I. Zhitomirsky, Electrodeposition of alginic acid and composite films, Colloids Surf. A Physicochem. Eng. Asp. 328 (2008) 73–78, https://doi.org/10.1016/j.colsurfa.2008.06.019.

[18] M. Chelly, S. Chelly, R. Zribi, H. Bouaziz-Ketata, R. Gdoura, N. Lavanya, G. Veerapandi, C. Sekar, G. Neri, Synthesis of silver and gold nanoparticles from Rumex roseus plant extract and their application in electrochemical sensors, Nanomaterials 11 (2021) 739.

[19] A.J. Bard, L.R. Faulkner, Fundamentals and applications, in: Electrochemical Methods, second ed., Wiley, New York, 2001, pp. 580–632.

[20] J. Soleymani, D. Perez-Guaita, M. Hasanzadeh, N. Shadjou, A. Jouyban, Materials and methods of signal enhancement for spectroscopic whole blood analysis: novel research overview, TrAC, Trends Anal. Chem. 86 (2017) 122–142, https://doi.org/10.1016/j.trac.2016.10.006.

[21] J. Soleymani, M. Hasanzadeh, M. Eskandani, M. Khoubnasabjafari, N. Shadjou, A. Jouyban, Electrochemical sensing of doxorubicin in unprocessed whole blood, cell lysate, and human plasma samples using thin film of poly-arginine modified glassy carbon electrode, Mater. Sci. Eng. C 77 (2017), https://doi.org/10.1016/j.msec.2017.03.257.

[22] M. Hasanzadeh, N. Shadjou, Electrochemical nanobiosensing in whole blood: recent advances, TrAC, Trends Anal. Chem. 80 (2016) 167–176, https://doi.org/10.1016/j.trac.2015.07.018.

[23] J. Fei, X. Wen, Y. Zhang, L. Yi, X. Chen, H. Cao, Voltammetric determination of trace doxorubicin at a nano-titania/nafion composite film modified electrode in the presence of cetyltrimethylammonium bromide, Microchim. Acta 164 (2009) 85–91, https://doi.org/10.1007/s00604-008-0037-y.

[24] M. Hasanzadeh, N. Hashemzadeh, N. Shadjou, J. Eivazi-Ziaei, M. Khoubnasabjafari, A. Jouyban, Sensing of doxorubicin hydrochloride using graphene quantum dot modified glassy carbon electrode, J. Mol. Liq. (2016).

[25] A. Peng, H. Xu, C. Luo, H. Ding, Application of a disposable doxorubicin sensor for direct determination of clinical drug concentration in patient blood, Int. J. Electrochem. Sci. 11 (2016) 6266–6278, https://doi.org/10.20964/2016.07.38.

[26] E. Haghshenas, T. Madrakian, A. Afkhami, Electrochemically oxidized multiwalled carbon nanotube/glassy carbon electrode as a probe for simultaneous determination of dopamine and doxorubicin in biological samples, Anal. Bioanal. Chem. 408 (2016) 2577–2586.

[27] M. Taei, F. Hasanpour, H. Salavati, S. Mohammadian, Fast and sensitive determination of doxorubicin using multi-walled carbon nanotubes as a sensor and CoFe2O4 magnetic nanoparticles as a mediator, Microchim. Acta 183 (2016) 49–56, https://doi.org/10.1007/s00604-015-1588-3.

[28] R. Hajian, Z. Tayebi, N. Shams, Sensitive determination of doxorubicin in plasma and study on doxorubicin-DNA interactions using platinum electrode modified multi-walled carbon nanotubes, J Pharm Anal (2016).

[29] J. Soleymani, M. Hasanzadeh, N. Shadjou, M. Khoubnasab Jafari, J. V. Gharamaleki, M. Yadollahi, A. Jouyban, A new kinetic-mechanistic approach to elucidate electrooxidation of doxorubicin hydrochloride in unprocessed human fluids using magnetic graphene based nanocomposite modified glassy carbon electrode, Mater. Sci. Eng. C 61 (2016) 638–650, https://doi.org/10.1016/j.msec.2016.01.003.

[30] M. Ehsani, J. Soleymani, M. Hasanzadeh, Y. Vaez-Gharamaleki, M. Khoubnasabjafari, A. Jouyban, Sensitive monitoring of doxorubicin in plasma of patients, MDA-MB-231 and 4T1 cell lysates using electroanalysis method, J. Pharm. Biomed. Anal. 192 (2021), 113701, https://doi.org/10.1016/j.jpba.2020.113701.